JACS
JOURNAL OF THE AMERICAN CHEMICAL SOCIETY

Article

pubs.acs.org/JACS

Dramatic Differences in Aggregation-Induced Emission and Supramolecular Polymerizability of Tetraphenylethene-Based Stereoisomers

Hui-Qing Peng,[†,‡] Xiaoyan Zheng,[†] Ting Han,[†,‡] Ryan T. K. Kwok,[†,‡] Jacky W. Y. Lam,[†,‡] Xuhui Huang,[†] and Ben Zhong Tang*[,†,‡,§]

[†]Department of Chemistry, Hong Kong Branch of Chinese National Engineering Research Center for Tissue Restoration and Reconstruction, Institute of Molecular Functional Materials, Institute for Advanced Study, State Key Laboratory of Neuroscience, Division of Biomedical Engineering and Division of Life Science, The Hong Kong University of Science and Technology, Clear Water Bay, Kowloon, Hong Kong 999077, China

[‡]Guangdong Provincial Key Laboratory of Brain Science, Disease and Drug Development, HKUST-Shenzhen Research Institute, Nanshan, Shenzhen 518057, China

[§]Guangdong Innovative Research Team, SCUT-HKUST Joint Research Laboratory, State Key Laboratory of Luminescent Materials and Devices, South China University of Technology, Guangzhou, Guangdong 510640, China

Supporting Information

ABSTRACT: Geometric (*Z*)- and (*E*)-isomers play important but different roles in life and material science. The design of new (*Z*)-/(*E*)- isomers and study of their properties, behaviors, and interactions are crucially important in molecular engineering. However, difficulties with their separation and structure confirmation limit their structural diversity and functionality in scope. In the work described herein, we successfully synthesized pure isomers of ureidopyrimidinone-functionalized tetraphenylethenes ((*Z*)-TPE-UPy and (*E*)-TPE-UPy), featuring both the aggregation-induced emission characteristic of tetraphenylethene and the supramolecular polymerizability of ureidopyrimidinone. Their structures were confirmed by 2D COSY and NOESY NMR spectroscopies. The two isomers show distinct fluorescence in the aggregate state: (*Z*)-TPE-UPy exhibits green emission, while its (*E*)-counterpart is blue-emitting. The cavity formed by the two ureidopyrimidinone groups of (*Z*)-TPE-UPy makes it suitable for Hg^{2+} detection, and the high-molecular-weight polymers prepared from (*E*)-TPE-UPy can be used to fabricate highly fluorescent fibers and 2D/3D photopatterns from their chloroform solutions.

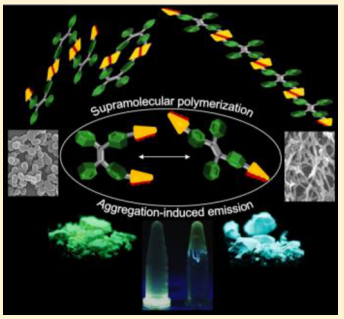

INTRODUCTION

Molecular engineering plays a crucial role in creating new functional materials, from the design to the study of their properties, behaviors, and interactions.[1,2] This "bottom-up" approach discloses how alteration of molecular structure affects the molecular packing and self-organization and works well to manipulate the function of a highly complex system. Synthetic chemists have modified numerous molecular structures to construct functional systems for chemical sensing,[3−6] biological imaging,[7−10] optical materials,[11−16] biological medicine,[17−19] and so on.[20] However, chemical modifications are sometimes time-consuming and costly. Additionally, a slight difference in molecular formula may affect the intrinsic molecular properties. Controlling the spatial configuration of one molecule is a potentially alternative strategy to tune the macroscopic properties of its corresponding functional materials.[21−28] Geometric (*Z*)- and (*E*)-isomers of molecules with carbon−carbon double bonds possess identical molecular formulas but different configurations and have been found to play different roles in life and material science. For instance, (*Z*)-tamoxifen is a weak estrogen agonist, but its (*E*)-cousin behaves as an effective estrogen antagonist for curing breast cancer.[29] Oligo(phenylene vinylene)s are an important class of π-conjugated optoelectronic materials, and their electron- and hole-transport properties are highly sensitive to the stereo-structures.[30] Thus, the design of new stereoisomers and elucidation of their structure−property−function relationships are crucially important in molecular engineering.

Tetraphenylethene (TPE) and its derivatives are well-suited for such studies because bifunctionalized TPE with (*Z*)- and (*E*)-configurations can be readily prepared by McMurry coupling of benzophenone carrying one functional group. Additionally, they exhibit aggregation-induced emission (AIE) properties with efficient light emission in the aggregate state.[31] This phenomenon overcomes the problem of aggregation-caused quenching of traditional fluorophores and enables functionalized TPE derivatives to find a wide range of highly technological applications in photoelectronic devices,[14,32−35] fluorescent sensing,[36−40] and supramolecular optical materials.[41−47] Because of the above-mentioned advantages, scientists have made efforts to separate and study TPE stereo-

Received: June 5, 2017
Published: July 10, 2017

DOI: 10.1021/jacs.7b05792
J. Am. Chem. Soc. 2017, 139, 10150−10156

isomers.[48−52] A pair of pure isomers have been synthesized for deciphering the mechanism of the AIE process,[48] while a few other isomers have been reported for exploring their distinguished biological applications.[50,51] The structural diversity and functionality of TPE stereoisomers are, however, still limited and less studied in detail. This may be due to their difficult separation and structure confirmation, which normally require the use of single-crystal X-ray crystallography.

Supramolecular polymers, which are formed by linking low-molecular-weight units by hydrogen bonding, $\pi-\pi$ interactions, and other reversible non-covalent interactions, play important roles in material science due to their unique mechanical properties and also reversibility, attributed to the dynamic nature of non-covalent interactions.[53−61] Whereas many supramolecular polymers with various structures and morphologies have been developed,[41−47,62] those fabricated from pure (*Z*)- and (*E*)-isomers of TPE, to the best of our knowledge, have not yet been explored. In this work, we report supramolecular polymers constructed by quadruple hydrogen bonding in pure stereoisomers of ureidopyrimidinone (UPy)-functionalized tetraphenylethenes ((*Z*)-TPE-UPy and (*E*)-TPE-UPy, Scheme 1). The isomers can be separated

Scheme 1. Synthesis and Schematic Representation of (*Z*)-TPE-UPy and (*E*)-TPE-UPy

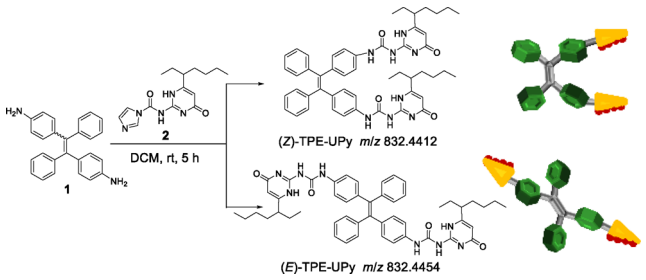

macroscopically by column chromatography in high yields. The structures of (*Z*)- and (*E*)-TPE-UPy were confirmed by 2D COSY and NOESY NMR spectroscopies. The two molecules show distinct fluorescence in the aggregate state: (*Z*)-TPE-UPy exhibits green emission, while its (*E*)-counterpart is blue-emitting. This difference inspired us to study their photophysical properties and supramolecular polymerizabilities. Distinct morphologies of particles and nanofibers were obtained by self-assembly of (*Z*)- and (*E*)-TPE-UPy, respectively. Our results are rationalized by the spatial configuration of TPE, which directs different supramolecular polymerizability and molecular packing of the isomers. The heteroatom-containing cavity offered by the two UPy groups of (*Z*)-TPE-UPy makes it suitable for Hg^{2+} coordination. In contrast, the high-molecular-weight polymers prepared from (*E*)-TPE-UPy permit us to obtain highly fluorescent fibers and 2D/3D photopatterns from their chloroform solutions.

RESULTS AND DISCUSSION

As a proof-of-concept, we incorporated 2-ureido-4[1*H*]-pyrimidinone (UPy) into TPE-based isomers to endow them with supramolecular polymerizability. This quadruple hydrogen-bonding motif was developed by Meijer[63] and has been widely used for supramolecular polymers due to its strong binding strength, association constant (5.7×10^7 M^{-1} in $CHCl_3$), and directionality. Molecules with two or more UPy units usually form supramolecular polymers through a ring−chain or isodesmic polymerization mechanism.[64] (*Z*)-TPE-UPy and (*E*)-TPE-UPy were prepared by a two-step reaction route (Scheme 1). First, McMurry coupling of 4-aminobenzophenone gave 1,2-(4-aminophenyl)-1,2-diphenylethane (**1**). Its isomers could be separated by column chromatography. However, as confirmed by thin-layer chromatography (TLC), they undergo isomerization during storage at room temperature. Reaction of an isomeric mixture of **1** with UPy precursor **2**[65] without the addition of any reactants gave (*Z*)- and (*E*)-TPE-UPy. Detailed procedures for their synthesis are provided in the Supporting Information (SI). Two separate spots were observed on the TLC plate using 5% methanol in dichloromethane as running solvent. The upper and lower spots were separated by column chromatography and characterized by NMR and mass spectroscopies (Figures S1−S8). The same *m*/*z* values in their mass spectra suggest that they are isomers (Figures S1 and S2). Both TPE-UPy isomers were very stable, undergoing no isomerization at room temperature, presumably due to the high activation barrier caused by their large structural difference. This provides good opportunities for studying their structures, properties, and related functionalities.

For correct assignment of the phenyl proton resonances, $^1H-^1H$ COSY spectroscopy was carried out. The $^1H-^1H$ COSY spectrum of the upper TLC is shown in Figure 1A. The doublet shift at δ 6.99 should correspond to the resonances of H_1 and H_2 protons due to the electron-donating property of the neighboring NH group. The resonance peak at δ 7.45 should stem from the H_3 and H_4 protons, as it has strong correlation with H_1 and H_2 (Figure 1A, solid black circles). After these assignments, the remaining peaks should belong to the proton resonances of the unsubstituted benzene ring. The integral of the multiplet at δ 7.08 suggests a relative proton number of 3, while that at δ 7.03 represents a proton number of 2. The strong correlations between protons at δ 7.08 suggest that they are H_5, H_6, and H_7, with through-bond coupling (Figure 1A, black dot circle). Accordingly, the resonance at δ 7.03 was assigned to H_8 and H_9. The full spectrum and those of the lower TLC fraction are given in Figures S9−S11. However, at this stage, correct assignment of the configuration of the products cannot be made. Fortunately, the distinguishable proton resonances between the UPy-substituted benzene ring (A) and the bare one (B) permit us to establish their through-space correlations. The NOESY spectrum of the lower TLC spot is shown in Figure 1B. As indicated by the cross-peaks in the black circles, nuclear Overhauser effect (NOE) was observed between protons H_3 and H_4 in ring A and between protons H_8 and H_9 in ring B. This effect arises only when ring A and ring B are spatially close to each other or, in other words, they are located on the same side of the central double bond. This result unambiguously proves the (*E*)-configuration of the lower TLC spot. No such NOE effect, however, was found in the upper TLC spot due to its (*Z*)-structure, which has the two rings far apart (Figure S12). The full NOESY spectra of the (*Z*)- and (*E*)-isomers are provided in Figures S13 and S14. Now, all the mass and NMR spectra in the SI can be readily assigned to respective isomers with full confidence.

After structural characterization, the optical properties of (*Z*)- and (*E*)-TPE-UPy were investigated. The UV spectra of (*Z*)- and (*E*)-TPE-UPy in chloroform are almost identical, with a maximum at 352 nm (Figure 2A). On the other hand, almost no signal was detected in their photoluminescence (PL) spectra. With a gradual increase of the hexane fraction in chloroform, intense emission was recorded (Figures 2B and

DOI: 10.1021/jacs.7b05792
J. Am. Chem. Soc. 2017, 139, 10150−10156

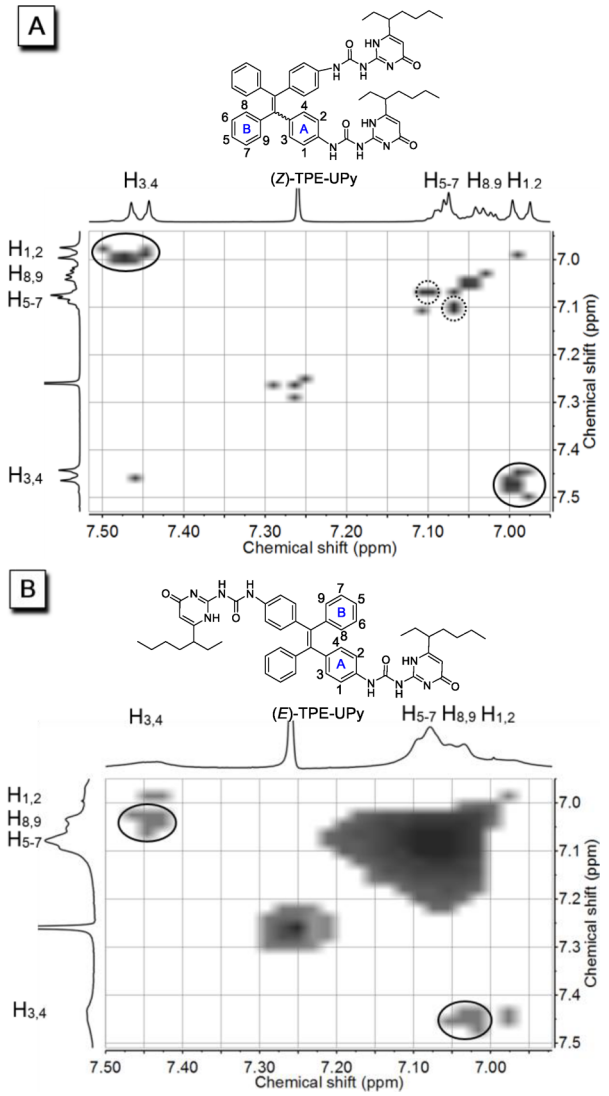

Figure 1. (A) Partial COSY spectrum of (*Z*)-TPE-UPy and (B) partial NOESY spectrum of (*E*)-TPE-UPy in $CDCl_3$.

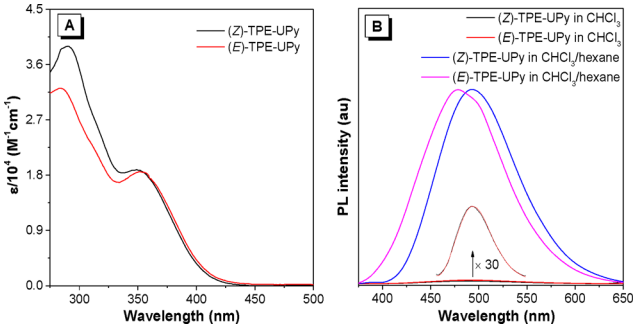

Figure 2. (A) UV spectra of (*Z*)- and (*E*)-TPE-UPy in $CHCl_3$ (10 μM). (B) Normalized PL spectra of (*Z*)- and (*E*)-TPE-UPy in $CHCl_3$ and $CHCl_3$/hexane (1:99, v/v), λ_{ex} = 350 nm.

S15A). Since (*Z*)- and (*E*)-TPE-UPy are insoluble in hexane, they formed aggregates in chloroform/hexane mixtures with high hexane fractions. Clearly, both isomers inherit the AIE characteristic of TPE. Their AIE feature is also verified by the fluorescence changes of (*Z*)-TPE-UPy in THF/water mixtures, as an example (Figure S15). Interestingly, the two isomers exhibit the same photophysical properties in the solution state but distinctly different aggregate-state emission. While (*Z*)-TPE-UPy shows a green fluorescence at 495 nm in a chloroform/hexane mixture (1/99, v/v), (*E*)-TPE-UPy is blue-emitting, with its PL spectrum peaked at 479 nm. An even larger difference between the PL maxima was found in their solid powers (Figure 3A).

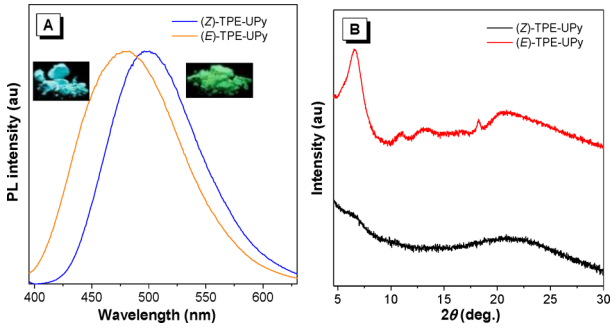

Figure 3. (A) Normalized PL spectra of (*Z*)- and (*E*)-TPE-UPy in the solid state, λ_{ex} = 350 nm. Inset: fluorescence photographs of (*Z*)- and (*E*)-TPE-UPy powders taken under 365 nm UV irradiation. (B) XRD diffractograms of the as-prepared powders of (*Z*)- and (*E*)-TPE-UPy.

It is reported that most AIEgens exhibit morphology-dependent emission: crystalline ones emit bluer fluorescence than their amorphous counterparts.[66−68] To check whether this is the cause for the different solid-state emissions of the stereoisomers, we checked their morphology by powder X-ray diffraction (XRD). As shown in Figure 3B, while the XRD diffractogram of (*E*)-TPE-UPy solid showed a diffraction peak at low angle, a diffuse halo was observed only in that of (*Z*)-TPE-UPy. This suggests that the former isomer packs in a somewhat layered fashion, while the latter one is amorphous in nature. The molecules of the (*E*)-isomer may adjust themselves to adopt a twisted conformation to fit into a solid lattice and maximize the interactions with their neighbors. Without such a constraint, the molecules of the (*Z*)-isomer may take a more planar conformation and thus show a redder fluorescence. The different solid-state PL of the isomers motivates us to study whether they also show different self-assembly behaviors. We believed that (*Z*)- and (*E*)-TPE-UPy may form polymers with different structures upon linking their molecules through quadruple hydrogen bonding.

The ^{1}H NMR spectra of (*Z*)- and (*E*)-TPE-UPy in $CDCl_3$ shown in Figures S3 and S6 show N−H proton resonances of the UPy units in a large downfield region, suggesting strong intermolecular UPy interactions through hydrogen bonding. Indeed, better-resolved resonance peaks were observed when CF_3COOD was added to the solution (Figures S4 and S7). Absorption peaks associated with hydrogen-bonded N−H stretching vibrations also verified the existence of hydrogen bonding (Figure S16). The polymerization mechanisms of the two stereoisomers were investigated by viscosity measurements. As shown in Figure 4A, a logarithmic plot of specific viscosity versus logarithm of concentration was linear for (*Z*)-TPE-UPy, with a slope of 1.1 at concentration below 160 mM, revealing the presence of non-interacting assemblies whose sizes are roughly constant (e.g., cyclic dimer). A slope of 3.9 was obtained at concentration above 160 mM, which suggests the formation of linear polymers whose molecular weights are concentration-dependent. The existence of a critical polymerization concentration indicates that the self-assembly of (*Z*)-

DOI: 10.1021/jacs.7b05792
J. Am. Chem. Soc. 2017, 139, 10150−10156

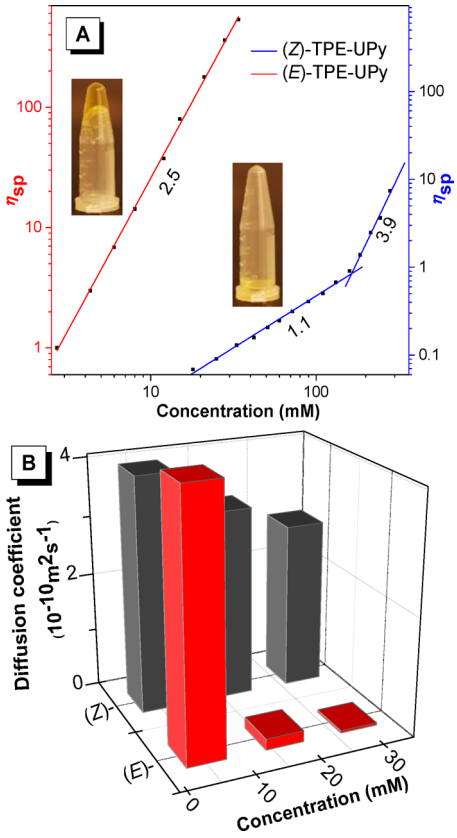

Figure 4. (A) Dependence of the specific viscosity of (*Z*)- and (*E*)-TPE-UPy in chloroform at 298 K on the solution concentration, shown with best-fit lines and slopes. Insets: photographs of solutions of stereoisomers at 50 mM. (B) Diffusion coefficients of (*Z*)- and (*E*)-TPE-UPy in chloroform solutions with different concentrations.

TPE-UPy occurs via a ring−chain polymerization mechanism (Figure 5). In contrast, the same plot for (*E*)-TPE-UPy gives a

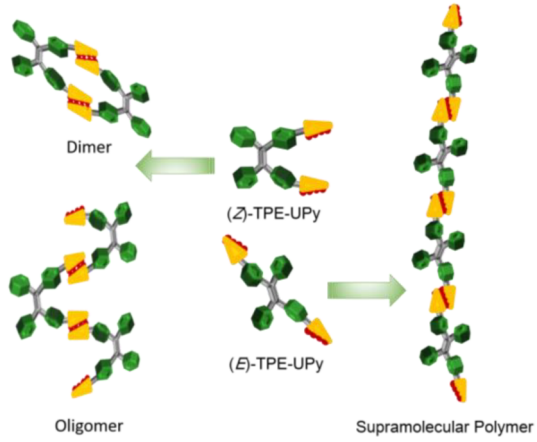

Figure 5. Schematic presentation of supramolecular polymerization by (*Z*)- and (*E*)-TPE-UPy.

slope of 2.5 in the whole concentration range. This implies that (*E*)-TPE-UPy can be polymerized even at very low solution concentration. This phenomenon conforms the isodesmic polymerization mechanism (Figure 5). Strikingly, the solution of (*E*)-TPE-UPy in chloroform is remarkably more viscous than that of (*Z*)-TPE-UPy under identical conditions (Figures 4A and S17). At the same mass fraction, the solution viscosity of (*E*)-TPE-UPy in chloroform is even higher than that of conventional polymers such as polystyrene and poly(methyl methacrylate) (Table S1). This provides excellent macroscopic processability to the supramolecular polymer for high-tech applications in photonic and electronic devices.

Analysis by diffusion-ordered spectroscopy (DOSY) on (*Z*)- and (*E*)-TPE-UPy in $CHCl_3$ gave results consistent with those of the viscosity measurements (Figure 4B). The weight-average diffusion coefficients (D) for supramolecular assemblies of (*Z*)-TPE-UPy formed in chloroform solutions at 12 and 24 mM are 3.24×10^{-10} and 2.82×10^{-10} m^2 s^{-1}, respectively (Figures S18 and S19). These values are slightly lower than that in the monomeric state in $CDCl_3$ + CF_3COOD (3.98×10^{-10} m^2 s^{-1}; Figure S20), revealing that a polymeric species with only low molecular weight was formed at such modest concentrations. By assuming a spherical shape and stable density of the self-assemblies, we estimated the degree of polymerization (DP) at 12 mM to be 1.85, indicating dimer formation.[69,70] This is further confirmed by the appearance of a signal at m/z = 1665.8953 g mol^{-1} ($[2M + H]^+$) in the ESI-MS spectrum (Figure S21). The diffusion coefficient for (*E*)-TPE-UPy decreases remarkably from 4.37×10^{-10} (monomeric state) to 1.86×10^{-11} and 3.98×10^{-12} m^2 s^{-1} (12 and 24 mM, polymeric state) (Figures S22−S24). This significant change verifies a high DP even at low solution concentration. According to a reported equation,[71,72] the DP of (*E*)-TPE-UPy is estimated to be 1655 at 12 mM, accounting for its highly viscous solution. A comparison of the supramolecular polymerizability of (*Z*)- and (*E*)-TPE-UPy clearly shows that the different TPE configurations strongly influence their self-assembly behaviors, which also change the macroscopic properties of the supramolecular polymers that are formed.

To gain more insight into the supramolecular polymerizability of (*Z*)- and (*E*)-TPE-UPy, we optimized the conformations of their dimers through quantum mechanics calculations according to density functional theory (DFT) at the B3LYP/3-21G* level by using the Gaussian 09 program. As shown in Figure 6, both the (*Z*)- and (*E*)-isomers can polymerize longitudinally based on the self-complementarity of the UPy units. For (*Z*)-TPE-UPy, both open dimer (I) and closed dimer (II) could be formed; however, the potential energy of dimer II is much lower than that of I (Table S2). With these optimized structures as building blocks, we can visualize the polymerization processes. In (*Z*)-TPE-UPy, the bulky UPy units are located on the same side of the double bond. This leads to large steric hindrance for UPy dimerization. Moreover, the energetically favorable dimer II terminated further self-assembly of itself. Thus, the supramolecular polymerizability of the (*Z*)-stereoisomer was low, and this explains why its solution shows a relatively low specific viscosity. However, the UPy units are located on opposite sides in (*E*)-TPE-UPy. As a result, the molecules suffer little constraint in UPy dimerization, and the resulting polymer exerts a high DP. Upon aggregation, the closed dimers or oligomers of (*Z*)-TPE-UPy in solution may arrange randomly and loosely due to their bent structures. In contrast, polymers formed by (*E*)-TPE-UPy in solution are long and linear in shape. This enables them to have a good packing in the aggregate state, which in turn affects the conformation of the chromophoric units and also the light emission of the aggregates/solids.

To further exploit the structure−property correlations, we investigated the morphologies of (*Z*)- and (*E*)-TPE-UPy

DOI: 10.1021/jacs.7b05792
J. Am. Chem. Soc. 2017, 139, 10150−10156

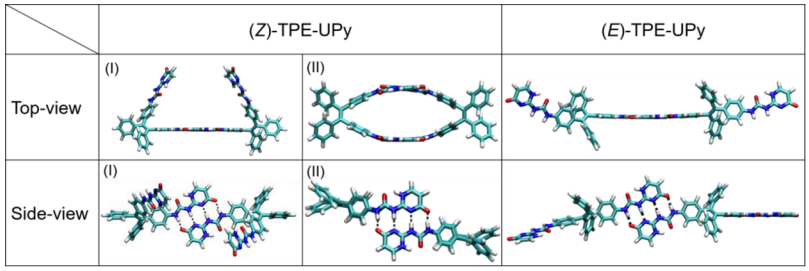

Figure 6. Optimized dimers formed by (*Z*)-TPE-UPy (I, open dimer; II, closed dimer) and (*E*)-TPE-UPy, calculated on the basis of the B3LYP/3-21G* method in the Gaussian 09 program. In each molecule, the 3-heptyl group was deleted and capped by a H-atom.

aggregates in chloroform/hexane mixtures (1:99, v/v) by scanning electron microscopy (SEM, Figures 7 and S25).

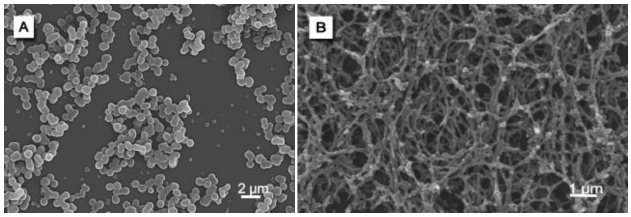

Figure 7. SEM images of (A) particles of (*Z*)-TPE-UPy formed in chloroform/hexane mixture (1:99, v/v) and (B) nanofibers of (*E*)-TPE-UPy formed in the same solvent mixture. Solution concentration: 100 μM.

Regular particles were observed from (*Z*)-TPE-UPy (Figure 7A). This is not unexpected, as polymerization of (*Z*)-TPE-UPy gives only low-molecular-weight species, whose further aggregation tends to form particles with low surface energy. In sharp contrast, cable-like structures were formed from (*E*)-TPE-UPy (Figure 7B). Such morphologies are believed to be formed by side-by-side association of linear polymers. The different aggregation morphologies exhibited by isomers are consistent with their difference in polymerizability, demonstrating that a subtle change in TPE configuration will have a great impact on the self-assembly behavior of the resulting molecule.

Molecular engineering seeks to understand and manipulate properties of macroscopic systems based on small molecular structures and behaviors. This strategy often produces new materials with specific functions. Here, we employed (*Z*)-TPE-UPy for Hg^{2+} sensing. The UPy units located on the same side of the molecule provide a cavity with coordination sites for metal ions. To demonstrate this possibility, heavy metal ions such as Cd^{2+}, Ni^{2+}, Zn^{2+}, Hg^{2+}, etc. were added respectively into (*Z*)-TPE-UPy solutions in THF/water (10 μM, 1/1, v/v). The obtained PL spectra suggest that (*Z*)-TPE-UPy can be used as a "turn-on" sensor for Hg^{2+} detection with high selectivity (Figure 8). The detection limit was calculated to be 3 ppm in the concentration range of 3.3−16.6 μM (Figure S26). However, (*E*)-TPE-UPy fails to offer such detection due to its very poor solubility in polar solvents.

The ESI-MS spectrum of the dye/metal ion complex shows peaks at m/z = 1033.4083 and 1069.3811, corresponding to $[M + Hg - H]^+$ and $[M + Hg + Cl]^+$, respectively (Figure S27), suggesting a stoichiometry of 1:1 between the organic and inorganic components. This result was supported by the Job plot of PL intensity against the molar fraction of Hg^{2+} (Figure S28). To determine the binding sites of Hg^{2+}, ^{1}H NMR titrations were carried out. Upon gradual addition of Hg^{2+}, the

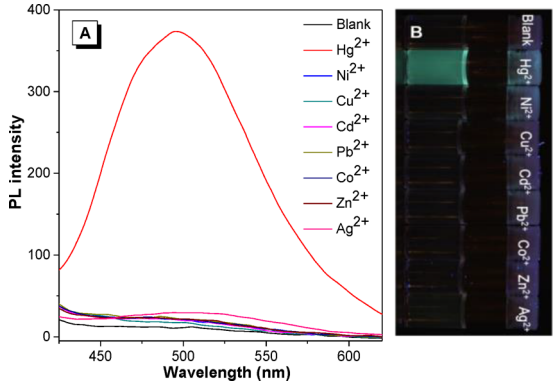

Figure 8. (A) PL spectra of (*Z*)-TPE-UPy in THF/water mixtures (10 μM; 1:1, v/v) with different metal ions (10 μM). (B) Fluorescence photos of the corresponding solutions taken under 365 nm UV irradiation.

resonance peaks at δ 9.65−11.20 became broader, but the integrals remained unchanged (Figure S29). This indicates that Hg^{2+} binds with the carbonyl oxygens or the imine nitrogen of the UPy units. Subsequently, the complex structure was proposed by quantum chemical calculations using the B3LYP/6-31G** (C, H, O, N) and lanl3DZ (Hg) methods in the Gaussian 09 program. The optimization combined with the experimental data suggests that each mercury ion is chelated by two imine nitrogen atoms and two ureido oxygen atoms, with Hg−N and Hg−O distances comparable with reported values (Figure S30).[73] Analysis of the Hg^{2+} coordination with (*Z*)-TPE-UPy may help us to develop new supramolecular materials with tunable hydrogen bonding and metal−ligand interactions.

The high viscosity owing to the high DP of (*E*)-TPE-UPy in $CHCl_3$ facilitates fiber fabrication. A rod-like fiber with regular diameter (400 nm) was drawn from its concentrated solution at 50 mM (Figure 9A). This fiber shows bright blue fluorescence when observed under fluorescence microscopy due to the aggregation-induced emission characteristic of the TPE unit (Figure 9B). Such fluorescent fibers formed by supramolecular polymerization of TPE derivatives may further extend the applications of AIEgens in optoelectronic devices. Conventional polymers have gained worldwide attention in material science, as their high molecular weights endow them with good film-forming capability and excellent macroscopic processability.[74−77] Here, in addition to fiber fabrication, we explored supramolecular polymers of (*E*)-TPE-UPy as new alternatives for photopattern generation. The (*E*)-isomer was dissolved in chloroform, and then a homogeneous and emissive film was formed on a silicon wafer by spin-coating. It is worth mentioning that the film prepared from (*Z*)-TPE-UPy was

DOI: 10.1021/jacs.7b05792
J. Am. Chem. Soc. 2017, 139, 10150−10156

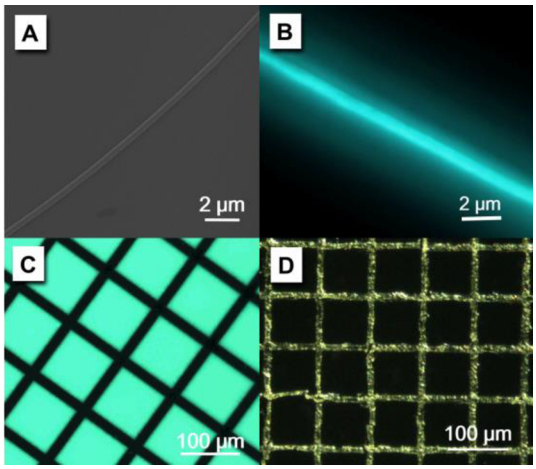

Figure 9. (A) SEM and (B) fluorescence images of fibers drawn from a solution of (*E*)-TPE-UPy in chloroform (50 mM). (C) Two-dimensional and (D) three-dimensional photopatterns taken under (C) UV light and (D) daylight generated by high-power UV irradiation of film prepared from (*E*)-TPE-UPy in $CHCl_3$ solution (24 mM).

phase-separated due to the low DP (Figure S31c). Next, the film was covered with a copper photomask and irradiated by high-power UV light (180 W) for 20 min. The emission of the irradiated regions (grid lines) was photobleached, while the covered parts (squares) remained emissive, generating a well-resolved 2D fluorescence pattern with sharp edges (Figure 9C). To confirm the photobleaching mechanism, the obtained pattern was washed with chloroform, which was a good solvent of the (*E*)-isomer. The fluorescent squares were removed by solvent, but the dark gridlines remained intact. This creates a 3D pattern with raised borders (Figure 9D). We believed that the high-power UV light induces cross-linking reaction of (*E*)-TPE-UPy, which decomposes the chromophore in (*E*)-TPE-UPy but causes the exposed regions to be insoluble.

CONCLUSIONS

In this work, pure stereoisomers of ureidopyrimidinone-functionalized tetraphenylethenes were isolated in high yields and characterized by different spectroscopic techniques. The aggregation-induced emission properties and supramolecular polymerizabilities of the stereoisomers depend strongly on the configuration of TPE. We demonstrated that the distinct polymerizability of (*Z*)-TPE-UPy and (*E*)-TPE-UPy affects the molecular packing, resulting in varied photophysical properties and morphologies in the aggregate/solid state. (*Z*)-TPE-UPy can function as a fluorescent sensor for specific detection of Hg^{2+} due to the heteroatom-containing cavity offered by the UPy unit. Fluorescent fiber as well as 2D and 3D photopatterns were fabricated from (*E*)-TPE-UPy, thanks to its outstanding supramolecular polymerizability. We believed that this work extends the family of stereoisomers available in molecular engineering with new structures and correlated morphologies and functionalities. Some previous examples of supramolecular polymers formed by other non-covalent interactions (e.g., host−guest or metal−ligand interactions) with TPE as chromophore have been reported. However, mixtures of (*Z*)-/(*E*)-isomers are generally used for self-assembly studies. Thus, this present study may entice supramolecular chemists to realize the importance of TPE configuration and develop well-defined functional supramolecular materials based on TPE stereoisomers. Considering that (*Z*)-/(*E*)-isomerization of TPE may occur under light or thermal treatment, the construction of smart materials using (*Z*)- and (*E*)-TPE-UPy, whose photophysical properties and corresponding morphologies could be controlled by external stimuli, is of great interest and will be carried out in the near future.

ASSOCIATED CONTENT

Supporting Information

The Supporting Information is available free of charge on the ACS Publications website at DOI: 10.1021/jacs.7b05792.

Materials and methods, synthetic procedures, characterization, and property investigation, including Figures S1−S31 and Tables S1 and S2 (PDF)

AUTHOR INFORMATION

Corresponding Author

*tangbenz@ust.hk

ORCID

Hui-Qing Peng: 0000-0001-6616-8197
Ting Han: 0000-0003-1521-6333
Xuhui Huang: 0000-0002-7119-9358
Ben Zhong Tang: 0000-0002-0293-964X

Notes

The authors declare no competing financial interest.

ACKNOWLEDGMENTS

We are grateful for financial support from National Basic Research Program of China (973 Program; 2013CB834701 and 2013CB834702), the University Grants Committee of Hong Kong (AoE/P-03/08), the Research Grants Council of Hong Kong (16301614, 16305015, C2014-15G, and N_HKUST604/14), and the Innovation and Technology Commission (ITC-CNERC14SC01). B.Z.T. is also grateful for support from the Guangdong Innovative Research Team Program of China (201101C0105067115) and the Science and Technology Plan of Shenzhen (JCYJ20160229205601482).

REFERENCES

(1) von Hippel, A. *Science* **1956**, *123*, 315.
(2) Ruiz-Pérez, L.; Messager, L.; Gaitzsch, J.; Joseph, A.; Sutto, L.; Gervasio, F. L.; Battaglia, G. *Sci. Adv.* **2016**, *2*, e1500948.
(3) Niu, L.-Y.; Guan, Y.-S.; Chen, Y.-Z.; Wu, L.-Z.; Tung, C.-H.; Yang, Q.-Z. *J. Am. Chem. Soc.* **2012**, *134*, 18928.
(4) Niu, L.-Y.; Chen, Y.-Z.; Zheng, H.-R.; Wu, L.-Z.; Tung, C.-H.; Yang, Q.-Z. *Chem. Soc. Rev.* **2015**, *44*, 6143.
(5) Paolesse, R.; Nardis, S.; Monti, D.; Stefanelli, M.; Di Natale, C. *Chem. Rev.* **2017**, *117*, 2517.
(6) Chen, Y.; Zhang, W.; Cai, Y.; Kwok, R. T. K.; Hu, Y.; Lam, J. W. Y.; Gu, X.; He, Z.; Zhao, Z.; Zheng, X.; Chen, B.; Gui, C.; Tang, B. Z. *Chem. Sci.* **2017**, *8*, 2047.
(7) Kim, H. M.; Cho, B. R. *Chem. Rev.* **2015**, *115*, 5014.
(8) Gu, X.; Zhao, E.; Zhao, T.; Kang, M.; Gui, C.; Lam, J. W. Y.; Du, S.; Loy, M. M. T.; Tang, B. Z. *Adv. Mater.* **2016**, *28*, 5064.
(9) Yang, Q.; Ma, Z.; Wang, H.; Zhou, B.; Zhu, S.; Zhong, Y.; Wang, J.; Wan, H.; Antaris, A.; Ma, R.; Zhang, X.; Yang, J.; Zhang, X.; Sun, H.; Liu, W.; Liang, Y.; Dai, H. *Adv. Mater.* **2017**, *29*, 1605497.
(10) Hong, G.; Antaris, A. L.; Dai, H. *Nat. Biomed. Eng.* **2017**, *1*, 0010.
(11) Forrest, S. R. *Nature* **2004**, *428*, 911.
(12) Yuan, W. Z.; Lu, P.; Chen, S.; Lam, J. W. Y.; Wang, Z.; Liu, Y.; Kwok, H. S.; Ma, Y.; Tang, B. Z. *Adv. Mater.* **2010**, *22*, 2159.

(13) Wang, X.; Wang, S.; Ma, Z.; Ding, J.; Wang, L.; Jing, X.; Wang, F. *Adv. Funct. Mater.* **2014**, *24*, 3413.
(14) Liu, Y.; Mu, C.; Jiang, K.; Zhao, J.; Li, Y.; Zhang, L.; Li, Z.; Lai, J. Y. L.; Hu, H.; Ma, T.; Hu, R.; Yu, D.; Huang, X.; Tang, B. Z.; Yan, H. *Adv. Mater.* **2015**, *27*, 1015.
(15) Dalapati, S.; Jin, E.; Addicoat, M.; Heine, T.; Jiang, D. *J. Am. Chem. Soc.* **2016**, *138*, 5797.
(16) Lu, Y.; Wang, J.; McGoldrick, N.; Cui, X.; Zhao, J.; Caverly, C.; Twamley, B.; Ó Máille, G. M.; Irwin, B.; Conway-Kenny, R.; Draper, S. M. *Angew. Chem., Int. Ed.* **2016**, *55*, 14688.
(17) Hu, Q.; Gao, M.; Feng, G.; Liu, B. *Angew. Chem., Int. Ed.* **2014**, *53*, 14225.
(18) Zhang, C.-J.; Wang, J.; Zhang, J.; Lee, Y. M.; Feng, G.; Lim, T. K.; Shen, H.-M.; Lin, Q.; Liu, B. *Angew. Chem., Int. Ed.* **2016**, *55*, 13770.
(19) Gui, C.; Zhao, E.; Kwok, R. T. K.; Leung, A. C. S.; Lam, J. W. Y.; Jiang, M.; Deng, H.; Cai, Y.; Zhang, W.; Su, H.; Tang, B. Z. *Chem. Sci.* **2017**, *8*, 1822.
(20) Wender, P. A.; Miller, B. L. *Nature* **2009**, *460*, 197.
(21) Yang, Q.-Z.; Huang, Z.; Kucharski, T. J.; Khvostichenko, D.; Chen, J.; Boulatov, R. *Nat. Nanotechnol.* **2009**, *4*, 302.
(22) Wang, J.; Kulago, A.; Browne, W. R.; Feringa, B. L. *J. Am. Chem. Soc.* **2010**, *132*, 4191.
(23) Xu, J.-F.; Chen, Y.-Z.; Wu, D.; Wu, L.-Z.; Tung, C.-H.; Yang, Q.-Z. *Angew. Chem., Int. Ed.* **2013**, *52*, 9738.
(24) Yan, X.; Xu, J.-F.; Cook, T. R.; Huang, F.; Yang, Q.-Z.; Tung, C.-H.; Stang, P. J. *Proc. Natl. Acad. Sci. U. S. A.* **2014**, *111*, 8717.
(25) Liu, Y.; Shan, T.; Yao, L.; Bai, Q.; Guo, Y.; Li, J.; Han, X.; Li, W.; Wang, Z.; Yang, B.; Lu, P.; Ma, Y. *Org. Lett.* **2015**, *17*, 6138.
(26) Robb, M. J.; Kim, T. A.; Halmes, A. J.; White, S. R.; Sottos, N. R.; Moore, J. S. *J. Am. Chem. Soc.* **2016**, *138*, 12328.
(27) Astumian, R. D. *Chem. Sci.* **2017**, *8*, 840.
(28) Zhang, J.; Ma, W.; He, X.-P.; Tian, H. *ACS Appl. Mater. Interfaces* **2017**, *9*, 8498.
(29) Katzenellenbogen, B. S.; Norman, M. J.; Eckert, R. L.; Peltz, S. W.; Mangel, W. F. *Cancer Res.* **1984**, *44*, 112.
(30) Nayyar, I. H.; Batista, E. R.; Tretiak, S.; Saxena, A.; Smith, D. L.; Martin, R. L. *J. Polym. Sci., Part B: Polym. Phys.* **2013**, *51*, 935.
(31) Mei, J.; Leung, N. L. C.; Kwok, R. T. K.; Lam, J. W. Y.; Tang, B. Z. *Chem. Rev.* **2015**, *115*, 11718.
(32) Zhao, Z.; Lam, J. W. Y.; Tang, B. Z. *J. Mater. Chem.* **2012**, *22*, 23726.
(33) Chen, L.; Jiang, Y.; Nie, H.; Lu, P.; Sung, H. H. Y.; Williams, I. D.; Kwok, H. S.; Huang, F.; Qin, A.; Zhao, Z.; Tang, B. Z. *Adv. Funct. Mater.* **2014**, *24*, 3621.
(34) Qin, W.; Yang, Z.; Jiang, Y.; Lam, J. W. Y.; Liang, G.; Kwok, H. S.; Tang, B. Z. *Chem. Mater.* **2015**, *27*, 3892.
(35) Yang, J.; Li, L.; Yu, Y.; Ren, Z.; Peng, Q.; Ye, S.; Li, Q.; Li, Z. *Mater. Chem. Front.* **2017**, *1*, 91.
(36) Kwok, R. T. K.; Leung, C. W. T.; Lam, J. W. Y.; Tang, B. Z. *Chem. Soc. Rev.* **2015**, *44*, 4228.
(37) Yan, X.; Wang, H.; Hauke, C. E.; Cook, T. R.; Wang, M.; Saha, M. L.; Zhou, Z.; Zhang, M.; Li, X.; Huang, F.; Stang, P. J. *J. Am. Chem. Soc.* **2015**, *137*, 15276.
(38) Guan, W.; Zhou, W.; Lu, C.; Tang, B. Z. *Angew. Chem., Int. Ed.* **2015**, *54*, 15160.
(39) Song, Z.; Kwok, R. T. K.; Ding, D.; Nie, H.; Lam, J. W. Y.; Liu, B.; Tang, B. Z. *Chem. Commun.* **2016**, *52*, 10076.
(40) Guan, W.; Wang, S.; Lu, C.; Tang, B. Z. *Nat. Commun.* **2016**, *7*, 11811.
(41) Jiang, B.-P.; Guo, D.-S.; Liu, Y.-C.; Wang, K.-P.; Liu, Y. *ACS Nano* **2014**, *8*, 1609.
(42) Song, N.; Chen, D.-X.; Qiu, Y.-C.; Yang, X.-Y.; Xu, B.; Tian, W.; Yang, Y.-W. *Chem. Commun.* **2014**, *50*, 8231.
(43) Yan, X.; Cook, T. R.; Wang, P.; Huang, F.; Stang, P. J. *Nat. Chem.* **2015**, *7*, 342.
(44) Ji, X.; Shi, B.; Wang, H.; Xia, D.; Jie, K.; Wu, Z. L.; Huang, F. *Adv. Mater.* **2015**, *27*, 8062.
(45) Tian, Y.; Yan, X.; Saha, M. L.; Niu, Z.; Stang, P. J. *J. Am. Chem. Soc.* **2016**, *138*, 12033.
(46) Zhou, Z.; Yan, X.; Saha, M. L.; Zhang, M.; Wang, M.; Li, X.; Stang, P. J. *J. Am. Chem. Soc.* **2016**, *138*, 13131.
(47) Yan, X.; Wang, M.; Cook, T. R.; Zhang, M.; Saha, M. L.; Zhou, Z.; Li, X.; Huang, F.; Stang, P. J. *J. Am. Chem. Soc.* **2016**, *138*, 4580.
(48) Wang, J.; Mei, J.; Hu, R.; Sun, J. Z.; Qin, A.; Tang, B. Z. *J. Am. Chem. Soc.* **2012**, *134*, 9956.
(49) Tseng, N.-W.; Liu, J.; Ng, J. C. Y.; Lam, J. W. Y.; Sung, H. H. Y.; Williams, I. D.; Tang, B. Z. *Chem. Sci.* **2012**, *3*, 493.
(50) Xu, L.; Zhu, Z.; Wei, D.; Zhou, X.; Qin, J.; Yang, C. *ACS Appl. Mater. Interfaces* **2014**, *6*, 18344.
(51) Zhang, C.-J.; Feng, G.; Xu, S.; Zhu, Z.; Lu, X.; Wu, J.; Liu, B. *Angew. Chem., Int. Ed.* **2016**, *55*, 6192.
(52) Fang, X.; Zhang, Y.-M.; Chang, K.; Liu, Z.; Su, X.; Chen, H.; Zhang, S. X.-A.; Liu, Y.; Wu, C. *Chem. Mater.* **2016**, *28*, 6628.
(53) Liu, Y.; Wang, Z.; Zhang, X. *Chem. Soc. Rev.* **2012**, *41*, 5922.
(54) Yu, G.; Jie, K.; Huang, F. *Chem. Rev.* **2015**, *115*, 7240.
(55) Yang, L.; Tan, X.; Wang, Z.; Zhang, X. *Chem. Rev.* **2015**, *115*, 7196.
(56) Qu, D.-H.; Wang, Q.-C.; Zhang, Q.-W.; Ma, X.; Tian, H. *Chem. Rev.* **2015**, *115*, 7543.
(57) Wei, P.; Yan, X.; Huang, F. *Chem. Soc. Rev.* **2015**, *44*, 815.
(58) Yan, X.; Xu, D.; Chi, X.; Chen, J.; Dong, S.; Ding, X.; Yu, Y.; Huang, F. *Adv. Mater.* **2012**, *24*, 362.
(59) Chi, X.; Yu, G.; Shao, L.; Chen, J.; Huang, F. *J. Am. Chem. Soc.* **2016**, *138*, 3168.
(60) Kang, Y.; Cai, Z.; Huang, Z.; Tang, X.; Xu, J.-F.; Zhang, X. *ACS Macro Lett.* **2016**, *5*, 1397.
(61) Qin, B.; Zhang, S.; Song, Q.; Huang, Z.; Xu, J.-F.; Zhang, X. *Angew. Chem., Int. Ed.* **2017**, *56*, 7639.
(62) Chi, X.; Zhang, H.; Vargas-Zúñiga, G. I.; Peters, G. M.; Sessler, J. L. *J. Am. Chem. Soc.* **2016**, *138*, 5829.
(63) Sijbesma, R. P.; Beijer, F. H.; Brunsveld, L.; Folmer, B. J. B.; Hirschberg, J. H. K. K.; Lange, R. F. M.; Lowe, J. K. L.; Meijer, E. W. *Science* **1997**, *278*, 1601.
(64) ten Cate, A. T.; Kooijman, H.; Spek, A. L.; Sijbesma, R. P.; Meijer, E. W. *J. Am. Chem. Soc.* **2004**, *126*, 3801.
(65) Keizer, H. M.; Sijbesma, R. P.; Meijer, E. W. *Eur. J. Org. Chem.* **2004**, *2004*, 2553.
(66) Yuan, W. Z.; Tan, Y.; Gong, Y.; Lu, P.; Lam, J. W. Y.; Shen, X. Y.; Feng, C.; Sung, H. H. Y.; Lu, Y.; Williams, I. D.; Sun, J. Z.; Zhang, Y.; Tang, B. Z. *Adv. Mater.* **2013**, *25*, 2837.
(67) Tong, J.; Wang, Y.; Mei, J.; Wang, J.; Qin, A.; Sun, J. Z.; Tang, B. Z. *Chem. - Eur. J.* **2014**, *20*, 4661.
(68) Zheng, X.; Peng, Q.; Zhu, L.; Xie, Y.; Huang, X.; Shuai, Z. *Nanoscale* **2016**, *8*, 15173.
(69) Xu, J.-F.; Huang, Z.; Chen, L.; Qin, B.; Song, Q.; Wang, Z.; Zhang, X. *ACS Macro Lett.* **2015**, *4*, 1410.
(70) Zhang, Q.-W.; Li, D.; Li, X.; White, P. B.; Mecinović, J.; Ma, X.; Ågren, H.; Nolte, R. J. M.; Tian, H. *J. Am. Chem. Soc.* **2016**, *138*, 13541.
(71) Folmer, B. J. B.; Sijbesma, R. P.; Meijer, E. W. *J. Am. Chem. Soc.* **2001**, *123*, 2093.
(72) Li, S.-L.; Xiao, T.; Xia, W.; Ding, X.; Yu, Y.; Jiang, J.; Wang, L. *Chem. - Eur. J.* **2011**, *17*, 10716.
(73) Mahjoub Ali, R.; Morsali, A.; Nejad Ramin, E. *Z. Naturforsch. B* **2004**, *59*, 1109.
(74) Deng, H.; Han, T.; Zhao, E.; Kwok, R. T. K.; Lam, J. W. Y.; Tang, B. Z. *Macromolecules* **2016**, *49*, 5475.
(75) Zhang, Y.; Zhao, E.; Deng, H.; Lam, J. W. Y.; Tang, B. Z. *Polym. Chem.* **2016**, *7*, 2492.
(76) Qiu, Z.; Han, T.; Kwok, R. T. K.; Lam, J. W. Y.; Tang, B. Z. *Macromolecules* **2016**, *49*, 8888.
(77) Han, T.; Zhao, Z.; Deng, H.; Kwok, R. T. K.; Lam, J. W. Y.; Tang, B. Z. *Polym. Chem.* **2017**, *8*, 1393.

DOI: 10.1021/jacs.7b05792
J. Am. Chem. Soc. 2017, 139, 10150−10156